SSRG International Journal of Electrical and Electronics Engineering
ISSN: 2348-8379/ https://doi.org/10.14445/23488379/IJEEE-V10I11P106

Volume 10 Issue 11, 56-67, November 2023

Original Article

Design and Comparative Performance Analysis of a Novel E-Core Fault-Tolerant Flux-Switching Motor with Multi-Permanent Magnet

Stephen Eduku[1], Joseph Sekyi-Ansah[2], Ebenezer Narh Odonkor[3], Alex Ewuam[4]

[1,3,4]*Department of Electrical and Electronics Engineering, Takoradi Technical University, Takoradi, Ghana.*
[2]*Department of Mechanical Engineering, Takoradi Technical University, Takoradi, Ghana.*

[1]*Corresponding Author : 5103180335@stmail.ujs.edu.cn*

Received: 15 September 2023 Revised: 17 October 2023 Accepted: 14 November 2023 Published: 30 November 2023

Abstract *- This research paper introduces a novel E-core designed Fault-Tolerant Flux-Switching Stator-PM (FTFSSPM) motor topology employing Multiple Permanent Magnet (MPM) materials. The primary objective of this design is to harness the synergy of the combined potential of different PMs as an alternative approach to address the high demand and cost volatility associated with Neodymium magnet (NdFeB) in PM motors. Additionally, incorporating E-Core design technology significantly enhances the fault-tolerant capabilities of the proposed motor topology, ensuring reliable performance even in the event of faults such as open circuits and short-circuits. The same motor topology is examined using various PM materials, including NdFeB, ferrite magnet (Y30BH), and Alnico magnet, to facilitate a fair and comprehensive design analysis. Furthermore, the results obtained through Finite Element Analysis (FEA) in the Ansys Maxwell electromagnet software reveal that the hybrid-PM combination of NdFeB and Y30BH delivers comparable and improved performance in terms of efficiency, output torque, torque density, and power density while maintaining minimal torque ripple when compared to the exclusive use of NdFeB. This outcome aligns with the research's overarching objectives. Notably, the hybrid-PM configuration involving NdFeB and Alnico demonstrates commendable electromagnet performance. However, the synergy between NdFeB and Y30BH proves superior and on par with the performance achieved solely with NdFeB.*

Keywords *- E-core, Stator-PM motor, Fault-tolerant, FEA, Flux-switching, Multi-PMs.*

1. Introduction

Rare-earth permanent magnet, namely, Neodymium magnet (NdFeB) designed motors, have become a common choice for electric vehicle traction drives owing to their notable efficiency and torque density. Nonetheless, concerns have arisen regarding the potential constraints in the supply or escalating costs of rare-earth magnets. As a result, the electric vehicle sector must explore alternative motor technologies that are not solely reliant on rare-earth magnets [1]. Therefore, this proposed research aims to explore the implementation of hybrid PM technology to substantially reduce the reliance on NdFeB magnets while maintaining optimal motor performance.

Nevertheless, Permanent Magnet (PM) motors have garnered significant attention and application in various fields within the extensive array of motor configurations. This popularity is attributed to their advantages, including increased torque density and operating efficiency, primarily stemming from the absence of field excitation winding [2]. Moreover, various electric motor types are employed for traction in Electric Vehicles (EVs), including the Interior Permanent Magnet Synchronous (IPMS) motor, Switch Reluctance (SR) motor, and DC motor. Among these, the Permanent Magnet Flux Switching (PMFS) Motor is suitable for high torque and power in electric vehicle traction applications.

Consequently, rare earth permanent magnets, particularly Neodymium, are commonly chosen as the primary flux source for electric design motors [3-5].Hence, there is a need to investigate alternative approaches for designing a flux-switching permanent magnet motor that substantially reduces neodymium magnet usage. This exploration aims to achieve a balance between preserving electromagnetic output performance and lowering overall motor costs.

In recent years, there have been significant technological advancements in electrical motors, particularly in the case of rotor Permanent Magnet (PM) motors and switched reluctance motors. However, it is important to note that

switched reluctance motors continue to face challenges related to power density, while rotor-PM motors still exhibit weaknesses in their mechanical design [6, 7].

Furthermore, it is worth noting that a switching flux motor designed with permanent magnets merges the benefits of Switched Reluctance (SR) motors and Permanent Magnet (PM) motors. Permanent Magnet (PM) materials are essential components in electrical motors, significantly impacting academia and various industries. They are valued for their distinctive attributes, including high torque density, power density, and efficiency. In conventional motor configurations, PMs are typically affixed to the rotating part of the motor.

However, this placement can lead to issues such as demagnetization, the risk of PM breakage, and the need for additional mechanical support, as indicated in [8-10]. Therefore, as demonstrated in [6, 11], a new type of brushless permanent magnet motor, a stator-PM motor, has been created. This design positions the permanent magnets within the stator, resulting in higher power density and enhanced mechanical robustness as key design advantages. The Flux Switching Motor (FSM) design incorporates excitation sources, including Permanent Magnets (PM) and field winding, within the static component (stator). In this configuration, the rotor is free from these excitation sources, contributing to the rotor's durability and simplicity, as discussed in [8, 12, 13].

Nonetheless, it is important to emphasize that the switched-flux PM motor represents an innovative approach to electrical motor design, offering distinct advantages compared to its traditional counterpart, the rotor-PM synchronous motor. Notable benefits of the switched-flux PM motor include higher output torque density, improved rotor durability, and enhanced overall efficiency, as previously outlined [14, 15]. However, it is essential to note that the primary economic constraint associated with Flux-Switching PM (FSPM) motors lies in their relatively lower utilization of permanent magnets. Furthermore, it has been acknowledged that the FSPM motor design displays a certain level of fault tolerance without relying on physical and magnetic segregation capabilities, thus impacting the fault-tolerant operational performance of the motor [16].

Consequently, it is paramount from a research perspective to enhance the fault-tolerant operational characteristics of the FSPM-designed motor. Therefore, it is a pressing research concern to elevate the fault-tolerant operational features of the FSPM-designed motor. Nonetheless, a commonly noted significant drawback in the design of fault-tolerant SFPM motors is the substantial use of the dominant magnet material (NdFeB) and its correlated high expenses [17-21]. Furthermore, pursuing innovative and alternative approaches to achieve a noteworthy reduction in the usage of rare-earth, high-performance permanent magnet materials in the design of FSPM motors while maintaining key performance factors like mean torque, efficiency, and power density has gained prominence in recent years. This research area has become increasingly competitive, primarily in response to the rising costs and volatility associated with permanent magnet materials, particularly Neodymium (NdFeB) [22, 23].

Afinowi et al. conducted a study examining the utilization of an alternative Permanent Magnet (PM) in FSPM motor design [6, 24]. Their findings revealed that FSPM motors using ferrite magnets produce a lower mean torque output when compared to those designed with NdFeB magnets. Nevertheless, the combination of ferrite and NdFeB magnets offers a distinctive approach to achieving comparable torque density and other performance metrics, thus presenting an attractive alternative to relying solely on the bulkier NdFeB magnets.

Furthermore, in response to the substantial surge in the cost and growing demand for rare-earth Permanent Magnet (PM) materials, there have been proposals for electric motor designs that utilize minimal rare-earth PMs, cost-effective ferrite magnets, or even no PM elements at all [25, 26]. These designs aim to maintain exceptional performance characteristics such as high efficiency and torque density, typically associated with motors designed using rare-earth PMs like NdFeB. Nevertheless, it is important to note that the current market for rare-earth PMs has become increasingly uncertain in terms of both pricing and availability [25, 27].

Moreover, within the realm of Permanent Magnet (PM) designed Flux Switching Motors (FSMs), both the permanent magnets and Armature Windings (AWs) are positioned in the stator, resulting in a sturdy rotor structure. Additionally, this configuration offers substantial power density, effective heat dissipation, and suitability for high-speed applications. However, it is worth noting that the significant reliance on rare-earth permanent magnets in this type of FSM contributes to an overall increase in the motor's cost [28]. Meanwhile, the availability of Permanent Magnet (PM) materials is diminishing over time, and the costs are steadily climbing [28-33].

In industrial applications, two primary classes of rare-earth Permanent Magnets (PMs) are widely used due to their powerful magnetic fields: Neodymium (NdFeB) and Samarium-Cobalt (SmCo). SmCo was the first rare-earth PM discovered and offers superior temperature stability and resistance to demagnetization but is less common than NdFeB due to its significantly higher cost and weaker magnetic performance. NdFeB is the most economically viable rare-earth PM widely adopted in various applications. However, the limited availability of rare-earth elements on

earth raises concerns about their future supply. Non-rare-earth Alnico PMs are emerging as competitive alternatives, known for their low-temperature sensitivity and high remnant (Br) flux density.

However, their low Coercivity (Hc) makes them vulnerable to demagnetization. In addition to Alnico, two common types of non-rare-earth magnets used in motors are ferrite PMs, primarily barium or strontium ferrite. Ferrite PMs are cost-effective, readily available, and possess higher coercivity but exhibit lower remnant flux density and maximum energy product [34, 35].

As the design configuration of an electric motor and the choice of permanent magnet materials exert a substantial impact on the electromagnetic performance of Permanent Magnet (PM) motors, this research paper introduces an E-core designed fault-tolerant flux-switching stator-PM motor with multi-magnet, namely, NdFeB, Y30BH, and Alnico, to demonstrate or assess its electromagnetic performance based on these magnet variations. This research paper's novelty or unique contribution can be categorized into two primary aspects.

Firstly, the unique feature or novelty of the proposed FTFSSPM motor topology lies in its capacity to effectively integrate synergy PMs. This allows it to compete favourably with the FTFSSPM motor configured solely with NdFeB magnets, showcasing a marginal increase in operating efficiency at a current angle of 0^{o}. This underscores the competitiveness of hybrid-PM motor technology over the exclusive use of NdFeB PM motor technology.

Secondly, integrating fault-tolerant teeth in the proposed FTFSSPM motor topology guarantees physical isolation of motor phase windings. If a fault occurs in one or two motor phase windings, the motor can sustain its operation with maintained or considerable design performance.

To facilitate a comprehensive analysis of the proposed design, the research paper is systematically organized into various sections as outlined below: Section 2 will present the materials, methods, and a detailed analysis of the proposed FTFSSPM motor topology. Section 3 will showcase the results and corresponding discussions through the Finite Element Analysis (FEA) conducted using ANSYS Maxwell electromagnetic software. Finally, in section 4, a comprehensive conclusion on the FTFSSPM motor topology will be drawn, ensuring clarity and ease of design replication.

2. Materials and Methods

To ensure a comprehensive understanding of the proposed FTFSSPM motor design, it is essential to provide a thorough account of the materials chosen for this research. A vital consideration in enabling a fair and meaningful comparison is the selection of M19_29G as the iron core material for both the stator and rotor core. This material boasts a proven track record in electric motor design and is renowned for its reliability. In addition, the three key Permanent Magnets (PMs) materials chosen for the proposed design are Neodymium magnet (NdFeB), Ferrite magnet (Y30BH), and Alnico magnet.

Table 1 provides specific details about these design materials and their corresponding specifications, facilitating an intuitive analysis. For precise performance evaluation and design optimization of electrical rotating motors, it is imperative to develop cost-effective mathematical models that maintain high accuracy.

However, a balance must be struck between the time-consuming process of creating an exact model capable of accurately simulating the motor performance and the economic feasibility of a less accurate model that reduces design costs. Notably, the Finite Element Method (FEM) is widely recognized as the most accurate and commonly employed approach among the various methods available for motor design. It is acknowledged that optimizing a motor's topology using FEA can be a time-intensive undertaking.

Furthermore, numerous electromagnetic design software packages exist for designing and analyzing Permanent Magnet (PM) motors, such as ANSYS Maxwell, MagNet, JMAG, and others. ANSYS Maxwell electromagnetic software is exceptionally advanced and widely adopted for designing and simulating PM motor topologies in 2D and 3D motor design. This research foundation is a basis for further exploration and analysis [36].

2.1. Motor Topology Design Analysis and Slot-Pole Synergy

The research introduces a five-phase E-core Fault-Tolerant Flux-Switching Stator-PM motor topology featuring various Multi-Permanent Magnet (MPM) configurations, as depicted in Figure 1. Figure 1(a) illustrates the motor with NdFeB magnets, Figure 1(b) with Y30BH ferrite magnets, and Figure 1(c) with Alnico magnets. Additionally, Figure 1(d) showcases the motor with a hybrid-PM setup using both NdFeB and Y30BH magnets, while Figure 1(e) presents a hybrid-PM configuration employing NdFeB and Alnico magnets.

The incorporation of the E-core design serves to enhance the fault-tolerant capabilities of the stator-PM flux-switching motor. The research maintains consistent motor topology specifications and winding arrangements, differing only in the PM arrangement for equitable analysis and comparison. The choice of a 10-stator slot and 19-rotor pole configuration for the proposed Fault-Tolerant Flux-Switching Stator-PM (FTFSSPM) motor is based on its ability to minimize cogging torque compared to the 10-slot and 18-pole design,

which exhibits a very low LCM despite having the highest winding factor. This selection is supported by prior testing and verification [37], which confirmed that the 10-slot and 19-pole combinations produce symmetrical back electromotive force, reducing cogging torque. In contrast, the 10-slot and 18-pole design leads to significant harmonic distortion. For reference, the slot diagram of the proposed FTFSSPM motor is depicted in Figure 2. However, Table 1 provides the specifications of the design parameters for easy comparison and analysis.

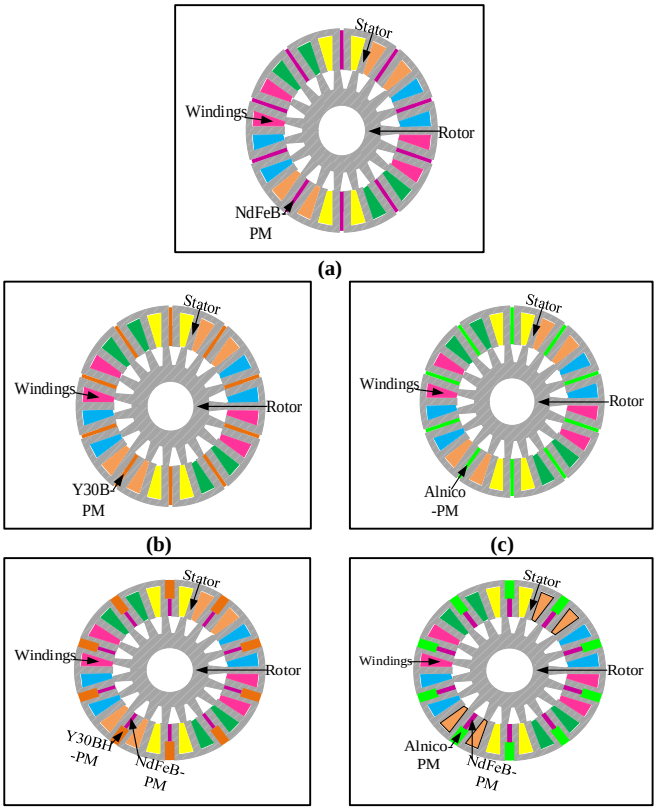

Fig. 1 Displays the various FTFSSPM motor topologies: (a) Solely NdFeB magnet configuration, (b) Solely Y30BH magnet configuration, (c) Solely Alnico magnet configuration, (d) Synergy of NdFeB and Y30BH magnet configuration, and (e) Synergy of NdFeB and Alnico magnet configuration.

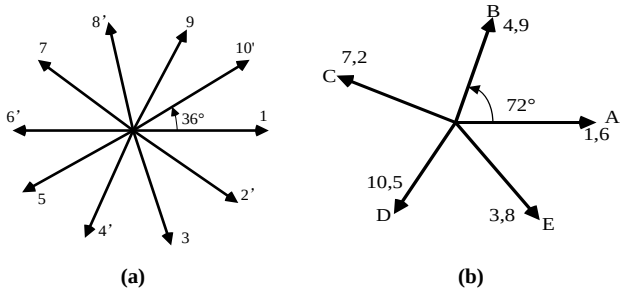

Fig. 2 presents the slot diagram for the 10-slot and 19-pole design, showcasing (a) the vectors of back electromotive force windings, and (b) the arrangement of phase windings.

Table 1. Design specification parameters of FTFSSPM motor topology

Symbol	Design Parameters	Specifications
Dso	Stator outer diameter (mm)	145
Dsi	Stator inner diameter (mm)	87
Dro	Rotor outer diameter (mm)	86.2
Dri	Rotor inner diameter (mm)	36
AL	Active axial length (mm)	60
Ag	Air-gap length (mm)	0.4
Nr	Rated speed (r/min)	1500
Ir	Rated current (A)	8.2
NBr	NdFeB PM remanence (T)	1.2
FBr	Ferrite PM remenance (T)	0.4
ABr	Alnico PM remanence (T)	1.1
Nt	Number of turns per slot	35
NP	Number of phases	5
	NdFeB PM material	NdFe35
	Ferrite PM material	Y30BH
	Alnico PM material	Alnico9

3. Results and Discussion

3.1. Design No-Load Performance Analysis

In this section of the research paper, the primary focus lies in analysing key attributes under the no-load operating condition. Specifically, it delves into electromotive force (Back-EMF), flux-linkage, and cogging torque. A comprehensive presentation of these characteristics is methodically conveyed in figures ranging from Figure 3 to Figure 6. Figure 3(a) illustrates that the motor design employing a Ferrite magnet (Y30BH) demonstrates a marginal increase in back-EMF.

This increase is noteworthy, as it is comparable to the back-EMF generated by the motor configuration utilizing Neodymium (NdFeB) magnets. It is worth noting that the motor with Alnico magnets, on the other hand, yields a slightly lower back-EMF compared to both NdFeB and Y30BH magnet-equipped designs. Additionally, it is crucial to emphasize that a higher back-EMF plays a significant role in boosting the electromagnetic torque production of the motor. Furthermore, it is worth noting that all the multi-PM motor configurations display a symmetrical (balanced) and sinusoidal back-EMF pattern. This characteristic is essential in ensuring the smooth operation of brushless AC motors by minimizing torque fluctuations, reducing acoustic noise, and minimizing vibration.

Moreover, as depicted in Figure 3(b), the back-EMF produced by the NdFeB motor topology surpasses that of the hybrid magnet configuration (NdFeB and Y30BH). This disparity in back-EMF is a clear advantage for the NdFeB motor design regarding output torque generation. However, as shown in Figure 3(c), the NdFeB-equipped motor topology consistently reveals a superior back-EMF compared to the configurations that combine NdFeB with Y30BH or Alnico magnets. This observation underscores its exceptional performance capability.

In Figure 4, the flux-linkage waveform of the Fault-Tolerant Flux-Switching Stator-PM (FTFSSPM) motor is depicted with a multi-PM configuration. Notably, all three PM motor setups demonstrate a balanced flux-linkage pattern, with the Y30BH motor configuration revealing a slightly higher flux-linkage when compared to the designs using NdFeB and Alnico magnets.

Furthermore, Figure 4(b) illustrates the flux linkage in the NdFeB motor design and the combined NdFeB-Y30BH and NdFeB-Alnico motor configurations. Additionally, it is noteworthy that the NdFeB motor design demonstrates flux linkage on par with the NdFeB-Y30BH combination. In contrast, the NdFeB-Alnico motor configuration reveals a slightly lower flux linkage than the above setup.

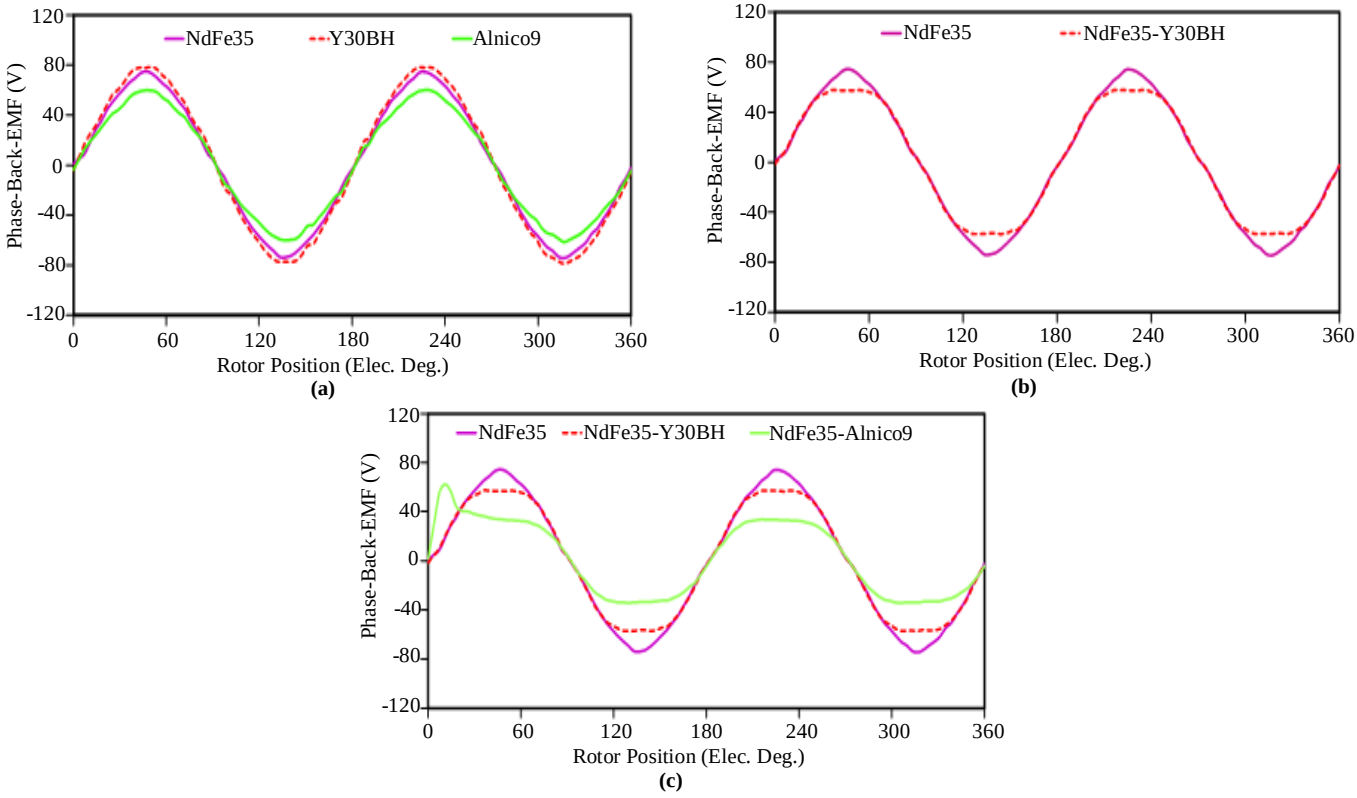

Fig. 3 Analysis of back-EMF waveforms in the FTFSSPM motor: (a) Back-EMF waveforms for NdFeB, Y30BH, and Alnico designs, (b) Back-EMF waveforms for NdFeB PM motor design and NdFeB-Y30BH configuration, and (c) Back-EMF waveforms for NdFeB motor design, NdFeB-Y30BH synergy, and NdFeB-Alnico synergy.

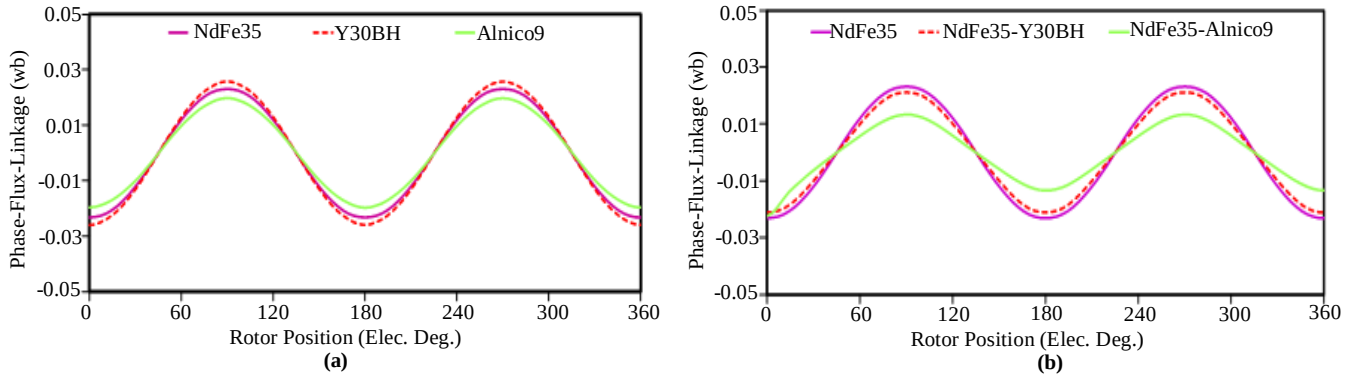

Fig. 4 Analysis of flux-linkage waveforms in FTFSSPM motor topologies: (a) NdFeB, Y30BH, and Alnico designs, and (b) NdFeB design, NdFeB-Y30BH combination, and NdFeB-Alnico synergy configurations.

As shown in Figures 5(a) and 5(b), the radial air-gap flux density of motor configurations using NdFeB, Y30BH, and Alnico magnets and the hybrid FTFSSPM motor configuration are illustrated.

In Figure 5(a), the radial flux density for the three selected PMs, NdFeB, Y30BH, and Alnico, exhibits similar waveform modulation, with NdFeB having the highest flux density. Figure 5(b) displays the radial induced air-gap flux density of the hybrid-PM technology, where NdFeB, the synergy of NdFeB-Y30BH, and the synergy of NdFeB exhibit comparable air-gap flux density, highlighting the competitiveness of different motor topologies based on distinct PM materials.

Figure 5(c) presents the circumferential (tangential) air-gap flux density of the three distinct PM motor configurations. In this case, the NdFeB design shows the highest air-gap flux density, while the Y30BH and Alnico PM motor configurations have comparable air-gap flux density.

Lastly, Figure 5(d) depicts the tangential air-gap flux density of the hybrid-PM motor configuration, where the NdFeB design, the synergy of NdFeB-Y30BH, and the synergy of NdFeB-Alnico motor configuration all display comparable air-gap flux density.

Cogging torque arises from the interplay between the rotor-mounted Permanent Magnets (PMs) and stator anisotropy, often stemming from the slotting in the stator. As a result, motors designed with closed slots or slotless stators remain unaffected by cogging torque.

To elaborate further, cogging torque results from the fluctuation in magnetic field energy caused by the position of the rotor as it rotates [38]. Brushless design Permanent Magnet (PM) motors are gaining popularity across various applications because of their exceptional attributes, such as high power density, efficiency, and dynamic performance, which often outperform other motor drive technologies.

Nevertheless, the issue of torque ripple in these motors remains a significant challenge, particularly in applications that demand precise speed and position control [39]. Therefore, addressing and minimising cogging during the initial design phase is crucial to ensure the electric motor operates smoothly and delivers optimal performance.

In Figure 6(a), the graph displays the cogging torque in the proposed FTFSSPM motor using different PM materials: NdFeB motor design, Y30BH motor design, and Alnico motor design. Notably, the NdFeB motor design shows a slightly higher cogging torque when compared to both the Y30BH motor design and the Alnico motor design.

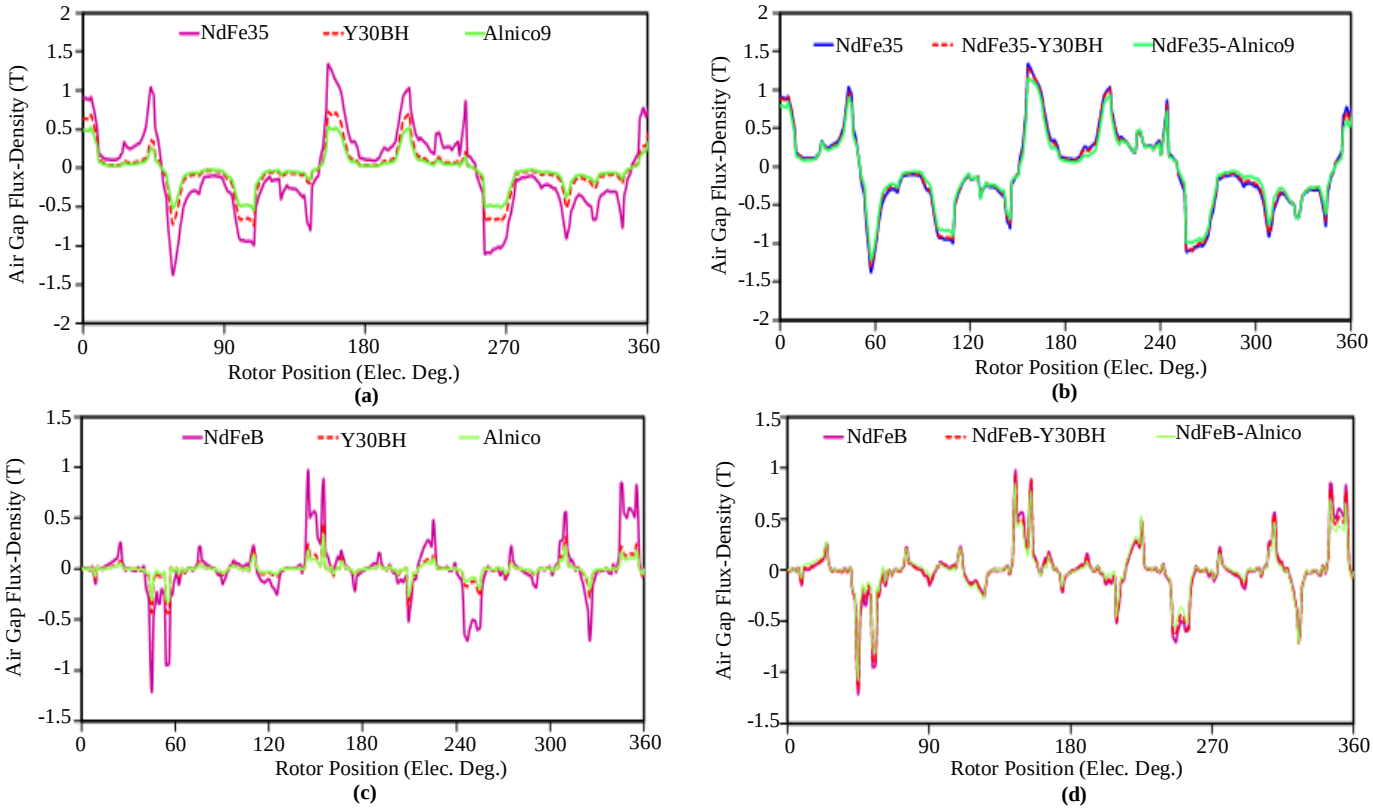

Fig. 5 presents an analysis of air-gap flux density, covering the following aspects: (a) Radial air-gap flux density for motor designs using NdFeB, Y30BH, and Alnico magnets, (b) Radial air-gap flux density for the hybrid-PM motor configuration, (c) Circumferential air-gap flux density for motor designs using NdFeB, Y30BH, and Alnico magnets, and (d) Circumferential air-gap flux density for the hybrid-PM motor configuration.

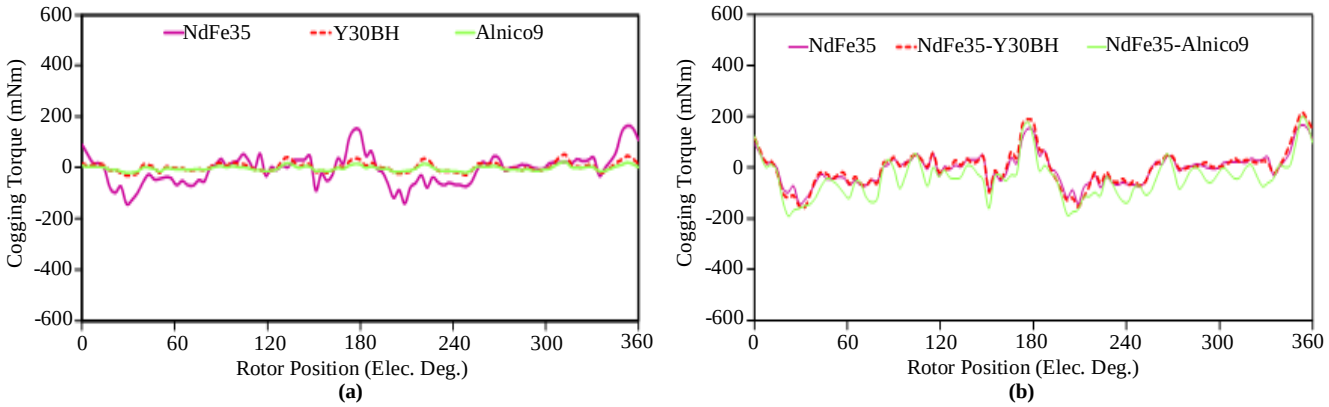

Fig. 6 Illustrates the cogging torque characteristics of the proposed FTFSSPM motor with multi-PM configurations: (a) Cogging torque waveforms for three PMs (NdFeB, Y30BH, and Alnico) motor topologies, and (b) Cogging torque waveform for the hybrid-PM motor topology.

Moving on to Figure 6(b), it illustrates the cogging torque in the hybrid-PM motor configuration. Remarkably, the hybrid-PM technology demonstrates comparable performance to using a large NdFeB magnet, which can contribute to increased motor costs. It's important to emphasize that the hybrid-PM motor topology holds promise and stands as a competitive option, particularly in applications where a motor solely reliant on NdFeB magnets might be economically challenging, thanks to its impressive electromagnetic performance.

3.2. Motor Configuration Performance Analysis at Load Condition

This section delves into the performance analysis of the FTFSSPM motor, considering an injected current with an amplitude of 8.2 amperes. To enhance clarity, Figure 7 presents torque performance analysis results obtained through the 2-D Finite Element Method (FEM).

The mean torque (Tavg) values for the FTFSSPM motor configurations are as follows: 8.09 Nm for the NdFeB motor design, 5.14 Nm for the Y30BH design, and 3.55 Nm for the Alnico motor design. Notably, the synergy of NdFeB and Y30BH yields an average torque of 7.72 Nm, while the NdFeB and Alnico synergy design results in 6.5 Nm.

Comparing the average torque of the NdFeB motor design to the NdFeB and Y30BH synergy design is a crucial aspect of this research, revealing a difference of 0.37 Nm. Consequently, it can be concluded that the NdFeB and Y30BH synergy design offers a comparable output torque.

Furthermore, the torque ripple for the NdFeB motor design and the NdFeB-Y30BH synergy design stands at 4.58% and 4.86%, respectively, at a current angle of 0 degrees. The determination of Torque Ripple (Tripp) for the proposed FTFSSPM motor topology can be computed using the provided equation.

For clarity and a more straightforward comparison of average torque, Figure 7(a) displays the average torque results for distinct PM motor configurations, namely the NdFeB, Y30BH, and Alnico motor designs. It's essential to emphasize that the NdFeB motor configuration achieved the highest average torque, followed by the Y30BH motor configuration, while the Alnico motor design exhibited the lowest average torque.

Furthermore, Figure 7(b) presents the average torque for the hybrid-PM motor configuration. As depicted in Figure 7(b), the synergy of the NdFeB and Y30BH motor configuration reveals a comparable average torque compared to the sole use of the NdFeB motor design.

In contrast, the synergy of NdFeB and Alnico exhibits the lowest average torque. While the average torque of the Alnico motor design topology is indeed lower than that of the NdFeB and Y30BH motor designs, it's worth noting that Alnico magnets exhibit strong Permanent Magnet (PM) memory characteristics.

This suggests that NdFeB and Y30BH may not possess the same PM retention or memory properties as Alnico magnets. Given that the NdFeB and Y30BH synergy has demonstrated promise as a competitive candidate in motor configurations alongside the NdFeB motor design, the waveforms of both the NdFeB motor design and the NdFeB and Y30BY synergy design have been included in Figure 7(c) to facilitate more precise and more intuitive analysis.

$$T_{ripple} = \frac{(T_{max} - T_{min})}{T_{avg}} x100\% = \frac{(T_{peak-to-peak})}{T_{avg}} x100\% \quad (1)$$

Where, Tmax signifies the maximum torque, Tmin represents the minimum torque, Tavg stands for the average torque obtained, and Tpeak-to-peak represents the peak-to-peak torque of the proposed design.

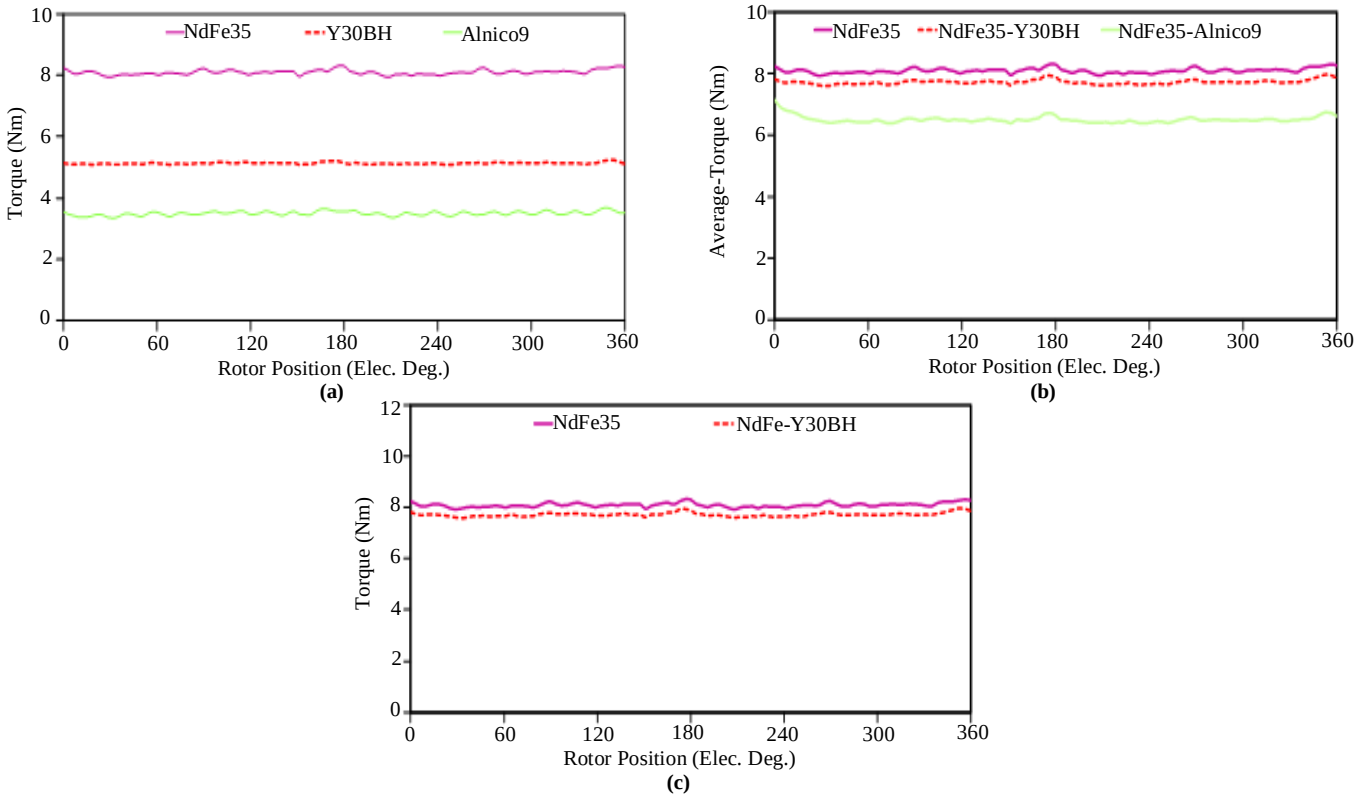

Fig. 7 Presents the analysis of average torque waveforms for the proposed FTFSSPM motor: (a) Displays the average torque waveforms for NdFeB, Y30BH, and Alnico motor designs, (b) Illustrates the average torque waveform for the hybrid-PM motor design, and (c) Shows the average torque waveform for the NdFeB motor design and the NdFeB-Y30BH synergy design.

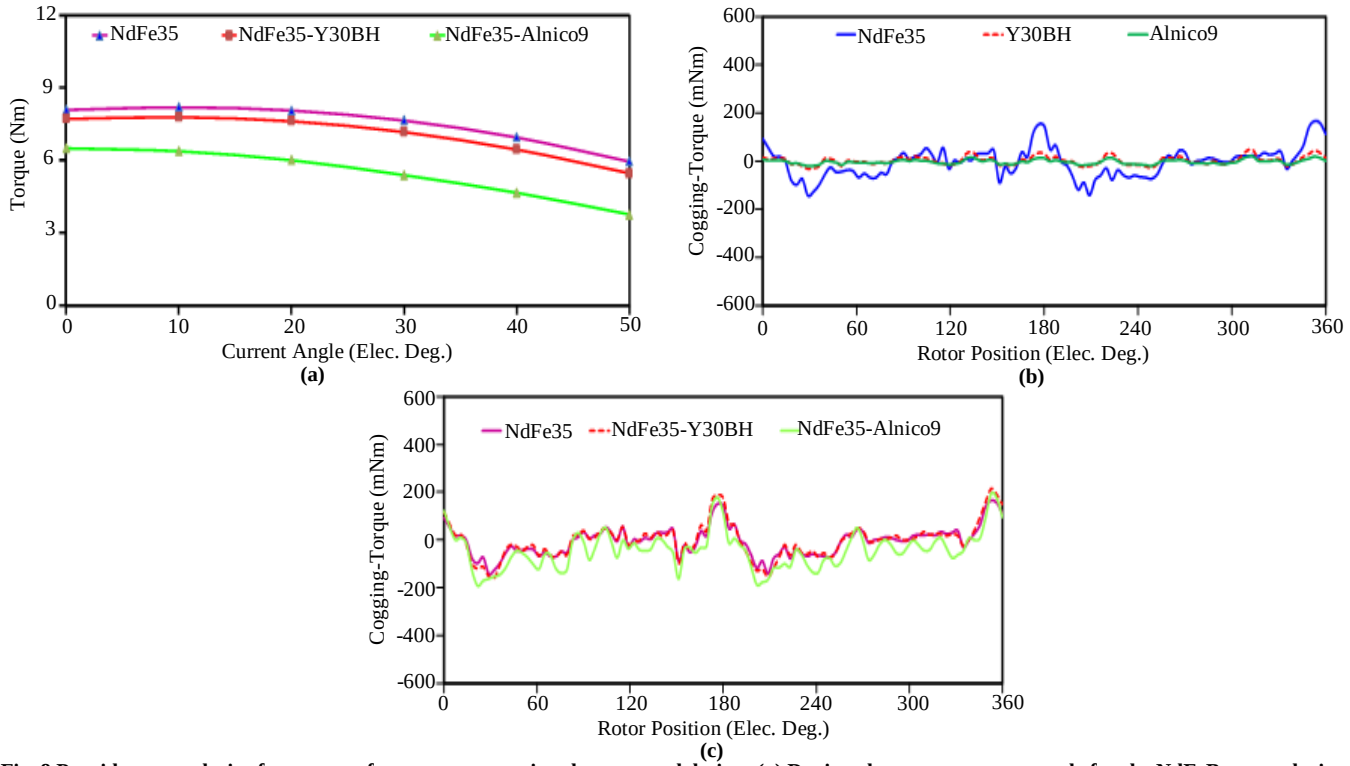

Fig. 8 Provides an analysis of torque performance concerning the proposed design: (a) Depicts the average torque angle for the NdFeB motor design, the NdFeB-Y30BH synergy design, and the NdFeB-Alnico synergy design, (b) Illustrates torque ripple at various current angles for the NdFeB, Y30BH, and Alnico motor designs, and (c) Shows torque ripple angle at different current angles for the hybrid-PM motor configuration.

In Figure 8, the analysis of the torque angle performance of the proposed FTFSSPM motor topology using multiple PMs is presented. As shown in Figure 8(a), the NdFeB motor configuration consistently produces slightly higher output torque at various current angles when compared to the NdFeB-Y30BH synergy design.

This is primarily due to the superior performance and the quantity of NdFeB magnets utilized in the NdFeB motor design, which surpasses the synergy configuration's NdFeB-Y30BH magnets. Furthermore, it's worth noting that the synergy of the NdFeB and Alnico motor design demonstrates the lowest output torque at various current angles compared to the NdFeB motor design and the NdFeB-Y30BH synergy design.

Furthermore, Figure 8(b) presents the torque ripple at different current angles for the three PM material motor topologies. The NdFeB motor design exhibits higher torque ripple or torque pulsation when contrasted with the Y30BH and Alnico motor designs. Moving on to Figure 8(c), it illustrates the torque ripple at various current angles for the hybrid-PM motor design. Here, the torque ripple behaviour highlights the hybrid-PM technology's comparable performance to the sole use of NdFeB motor design. This reinforces the notion that hybrid-PM technology holds promise as a design candidate, mainly when the aim is to reduce the volume of NdFeB magnets and consequently lower the motor's overall cost.

3.3. Core Losses and Design Efficiency Performance Comparison

Section C of this research paper explore PM and iron core losses along with their waveforms and analyzes the computed efficiency of the proposed FTFSSPM motor model. This analysis aims to enhance the comparison and reveal the effectiveness of the proposed FTFSSPM design, which incorporates multiple PMs. These losses were determined through 2-D FEM analysis, with a current angle of 0 degrees, and the detailed results are outlined in Table 2. These results are further substantiated by the waveforms of the NdFeB motor design, the NdFeB-Y30BH synergy design, and the NdFeB-Alnico synergy design shown in Figure 9.

However, it is evident from the findings presented in Figure 9(a) that the NdFeB motor topology exhibits the highest PM losses at various current angles, compared to the synergy of NdFeB and Y30BH design. Hence, it can be concluded that the hybrid-PM technology motors unveil minimal PM losses compared to the sole use of a NdFeB magnet. Additionally, it is noteworthy that the synergy of the NdFeB and Alnico configuration demonstrates the lowest PM losses.

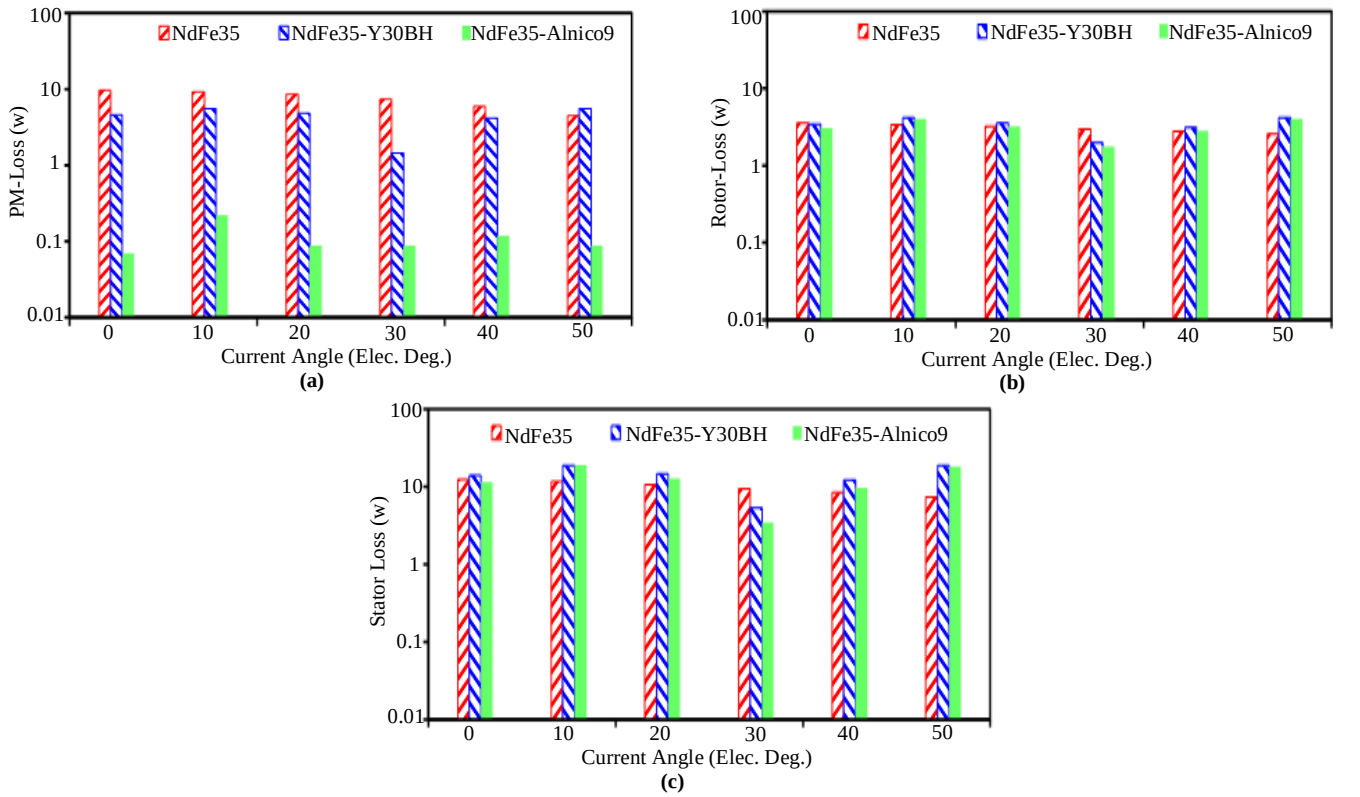

Fig. 9 Illustrates the analysis of PM and iron core losses at different current angles: (a) PM losses waveform, (b) Rotor losses waveform, and (c) Stator losses waveform.

Table 2. Core loss comparison of the FTFSSPM motors

Items	NdFe35	NdFe35-Y30BH	NdFeB-Alnico9
PM loss (W)	9.62	4.62	0.07
Rotor iron loss (W)	3.56	3.42	3.12
Stator iron loss (W)	12.49	13.96	11.62
Copper loss (W)	24.48	24.48	24.48

Furthermore, the results of rotor losses and stator losses based on the NdFeB motor design, the NdFeB-Y30BH synergy motor design, and the NdFeB-Alnico synergy motor design are presented in Figures 9(b) and 9(c). These results highlight that the proposed motor configuration with distinct PMs exhibits comparable rotor and stator losses. Moreover, the efficiency (η) of the proposed FTFSSPM motor, considering different PMs, can be calculated using the following formula:

$$\eta = \frac{T_{avg\omega}}{T_{avg\omega}+P_{cu}+P_{pm}+P_r+P_s} x100\% \text{ or}$$

$$\eta = 1 - \left(\frac{P_{Loss}}{P_{In}}\right) x100\% \quad (2)$$

Where, P_{Loss} represents the power loss within the motor, and Pin denotes the motor's input power.

Moreover, the design efficiency of the proposed FTFSSPM motor is 96. 17% for NdFeB motor configuration, 96.28% for the synergy of NdFeB and Y30BH motor configuration and 96.26% for the synergy NdFeB and Alnico motor configuration. Furthermore, it is imperative to highlight that the infinitesimal or slight difference in efficiency in both hybrid-PM motor configurations, namely synergy of NdFeB and Y30BH and synergy of NdFeB and Alnico are partly due to the high PM losses exhibited by the solely used NdFeB motor configuration. Hence, it can be concluded from the analysis mentioned above without doubt that the synergy of NdFeB and Y30BH motor configuration is a promising design candidate or choice to compute in applications where the solely used NdFeB motor configuration is required due to its high output electromagnetic performances such as torque, torque density, power density, and operating efficiency. To further buttress these findings, a graphical representation of the efficiencies for the NdFeB, NdFeB-Y30BH synergy, and NdFeB-Alnico synergy motor configurations is presented in Figure 10 for a more intuitive analysis.

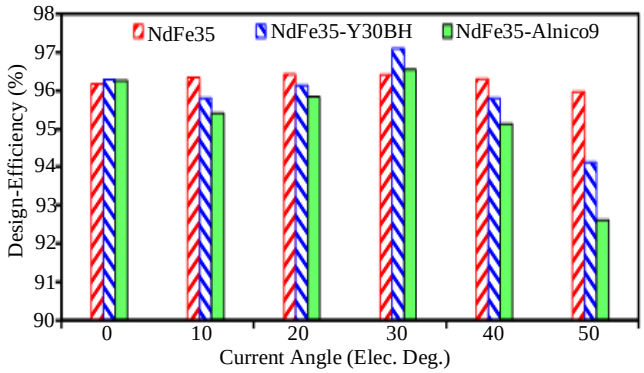

Fig. 10 Efficiency of the proposed FTFSSPM motor at distinct current angles

4. Conclusion

This paper introduces a novel E-core Fault-Tolerant Flux-Switching Stator-PM (FTFSSPM) motor featuring a multi-PM configuration. The primary objective is to reduce the heavy reliance on NdFeB magnets in flux-switching PM motors while preserving high electromagnetic torque and efficiency with minimal core losses and torque ripple.

Moreover, results obtained using Finite Element Method (FEM) analysis reveal that the hybrid-PM motor configuration, specifically the synergy of NdFeB and Y30BH motor design, offers comparable output performance when compared to the exclusive use of NdFeB magnets. However, for intuitive analysis and comparison, the average torque obtained at the current angle 0^o for the NdFeB motor, synergy of NdFeB and Y30BH motor and synergy of NdFeB and Alnico are 8.09 Nm, 7.72 Nm, and 6.5 Nm respectively, with a torque ripple of the NdFeB motor, synergy of NdFeB and Y30BH, and synergy of NdFeB and Alnico being 4.58%, 4.86%, and 11.78% respectively. Moreover, the efficiency of the NdFeB motor configuration, synergy of NdFeB and Y30BH motor configuration and synergy of the NdFeB and Alnico motor configuration are 96.17%, 96.29% and 96.26%, respectively.

References

[1] Maged Ibrahim, Lesedi Masisi, and Pragasen Pillay, "Design of Variable-Flux Permanent-Magnet Machines Using Alnico Magnets," *IEEE Transactions on Industry Applications*, vol. 51, no. 6, pp. 4482-4491, 2015. [CrossRef] [Google Scholar] [Publisher Link]

[2] Z.Q. Zhu et al., "Comparative Study of Partitioned Stator Machines with Different PM Excitation Stators," *IEEE Transactions on Industry Applications*, vol. 52, no. 1, pp. 199-208, 2016. [CrossRef] [Google Scholar] [Publisher Link]

[3] Syed Muhammad Naufal Bin Syed Othman et al., "Design and Analysis of Three Phase SegSta 12S-12P Permanent Magnet Flux Switching Machine," *2019 2nd International Conference on Computing, Mathematics and Engineering Technologies (iCoMET)*, Sukkur, Pakistan, pp. 1-4, 2019. [CrossRef] [Google Scholar] [Publisher Link]

[4] Ki-Chan Kim, "A Novel Method for Minimization of Cogging Torque and Torque Ripple for Interior Permanent Magnet Synchronous Motor," *IEEE Transactions on Magnetics*, vol. 50, no. 2, pp. 793-796, 2014. [CrossRef] [Google Scholar] [Publisher Link]

[5] Zhi Yang et al., "Comparative Study of Interior Permanent Magnet, Induction, and Switched Reluctance Motor Drives for EV and HEV Applications," *IEEE Transactions on Transportation Electrification*, vol. 1, no. 3, pp. 245-254, 2015. [CrossRef] [Google Scholar] [Publisher Link]

[6] Petrica Taras, Guang-Jin Li, and Zi Qiang Zhu, "Comparative Study of Fault-Tolerant Switched-Flux Permanent-Magnet Machines," *IEEE Transactions on Industrial Electronics*, vol. 64, no. 3, pp. 1939-1948, 2017. [CrossRef] [Google Scholar] [Publisher Link]

[7] Wenxiang Zhao et al., "Stator-Flux-Oriented Fault-Tolerant Control of Flux-Switching Permanent-Magnet Motors," *IEEE Transactions on Magnetics*, vol. 47, no. 10, pp. 4191-4194, 2011. [CrossRef] [Google Scholar] [Publisher Link]

[8] Basharat Ullah et al., "Performance Analysis of a Modular E-Shaped Stator Hybrid Excited Flux Switching Motor with Flux Gaps," *IEEE Access*, vol. 10, pp. 116098-116106, 2022. [CrossRef] [Google Scholar] [Publisher Link]

[9] Hao Chen, Ayman M. EL-Refaie, and Nabeel A.O. Demerdash, "Flux-Switching Permanent Magnet Machines: A Review of Opportunities and Challenges- Part I: Fundamentals and Topologies," *IEEE Transactions on Energy Conversion*, vol. 35, no. 2, pp. 684-698, 2020. [CrossRef] [Google Scholar] [Publisher Link]

[10] Aldo Boglietti et al., "Electrical Machine Topologies: Hottest Topics in the Electrical Machine Research Community," *IEEE Industrial Electronics Magazine*, vol. 8, no. 2, pp. 18-30, 2014. [CrossRef] [Google Scholar] [Publisher Link]

[11] Chunhua Liu et al., "Comparison of Stator-Permanent-Magnet Brushless Machines," *IEEE Transactions on Magnetics*, vol. 44, no. 11, pp. 4405-4408, 2008. [CrossRef] [Google Scholar] [Publisher Link]

[12] Lihong Mo, Tao Zhang, and Qing Lu, "Design and Analysis of an Outer-Rotor-Permanent-Magnet Flux-Switching Machine for Electric Vehicle Applications," *IEEE Transactions on Applied Superconductivity*, vol. 29, no. 2, pp. 1-5, 2019. [CrossRef] [Google Scholar] [Publisher Link]

[13] Enwelum I. Mbadiwe, and Erwan Bin Sulaiman, "Design and Optimization of Outer-Rotor Permanent Magnet Flux Switching Motor Using Transverse Segmental Rotor Shape for Automotive Applications," *Ain Shams Engineering Journal*, vol. 12, no. 1, pp. 507-516, 2021. [CrossRef] [Google Scholar] [Publisher Link]

[14] Yu Wang et al., "Improved Control Strategy for Fault-Tolerant Flux-Switching Permanent-Magnet Machine under Short-Circuit Condition," *IEEE Transactions on Power Electronics*, vol. 34, no. 5, pp. 4536-4557, 2019. [CrossRef] [Google Scholar] [Publisher Link]

[15] Amin Nobahari, Mehdi Aliahmadi, and Jawad Faiz, "Performance Modifications and Design Aspects of Rotating Flux Switching Permanent Magnet Machines: A Review," *IET Electric Power Applications*, vol. 14, no. 1, pp. 1-15, 2020. [CrossRef] [Google Scholar] [Publisher Link]

[16] Ming Cheng et al., "Overview of Stator Permanent Magnet Brushless Machines," *IEEE Transactions on Industrial Electronics*, vol. 58, no. 11, pp. 5087-5101, 2011. [CrossRef] [Google Scholar] [Publisher Link]

[17] I.A.A. Afinowi et al., "Performance Analysis of Switched-Flux Machines with Hybrid NdFeB and Ferrite Magnets," *2014 17th International Conference on Electrical Machines and Systems (ICEMS)*, Hangzhou, China, pp. 3110-3116, 2014. [CrossRef] [Google Scholar] [Publisher Link]

[18] Alessandro Fasolo, Luigi Alberti, and Nicola Bianchi, "Performance Comparison between Switching-Flux and IPM Machines with Rare-Earth and Ferrite PMs," *2012 20th International Conference on Electrical Machines*, Marseille, France, pp. 731-737, 2012. [CrossRef] [Google Scholar] [Publisher Link]

[19] Toomas Vaimann et al., "Magnetic Properties of Reduced Dy NdFeB Permanent Magnets and Their Usage in Electrical Machines," *2013 Africon*, Pointe Aux Piments, Mauritius, pp. 1-5, 2013. [CrossRef] [Google Scholar] [Publisher Link]

[20] Silong Li, Yingjie Li, and Bulent Sarlioglu, "Performance Assessment of High-speed Flux-Switching Permanent Magnet Machine Using Ferrite and Rare Earth Permanent Magnet Materials," *Electric Power Components and Systems*, vol. 43, no. 6, pp. 711-720, 2015. [CrossRef] [Google Scholar] [Publisher Link]

[21] Hao Chen, Ayman M. EL-Refaie, and Nabeel A.O. Demerdash, "Flux-Switching Permanent Magnet Machines: A Review of Opportunities and Challenges - Part II: Design Aspects, Control, and Emerging Trends," *IEEE Transactions on Energy Conversion*, vol. 35, no. 2, pp. 699-713, 2020. [CrossRef] [Google Scholar] [Publisher Link]

[22] Tsarafidy Raminosoa et al., "Reduced Rare-Earth Flux-Switching Machines for Traction Applications," *IEEE Transactions on Industry Applications*, vol. 51, no. 4, pp. 2959-2971, 2015. [CrossRef] [Google Scholar] [Publisher Link]

[23] Hongsik Hwang, Sungwoo Bae, and Cheewoo Lee, "Analysis and Design of a Hybrid Rare-Earth-Free Permanent Magnet Reluctance Machine by Frozen Permeability Method," *IEEE Transactions on Magnetics*, vol. 52, no. 7, pp. 1-4, 2016. [CrossRef] [Google Scholar] [Publisher Link]

[24] I.A.A. Afinowi et al., "Switched-Flux Machines with Hybrid NdFeB and Ferrite Magnets," *COMPEL International Journal for Computation & Mathematics in Electrical & Electronic Engineering*, vol. 35, no. 2, pp. 456-472, 2016. [CrossRef] [Google Scholar] [Publisher Link]

[25] Ion Boldea et al., "Automotive Electric Propulsion Systems with Reduced or No Permanent Magnets: An Overview," *IEEE Transactions on Industrial Electronics*, vol. 61, no. 10, pp. 5696-5711, 2014. [CrossRef] [Google Scholar] [Publisher Link]

[26] Z.Q. Zhu, "Switched Flux Permanent Magnet Machines - Innovation Continues," *2011 International Conference on Electrical Machines and Systems*, Beijing, China, pp. 1-10, 2011. [CrossRef] [Google Scholar] [Publisher Link]

[27] Zhongze Wu et al., "Analysis and Suppression of Induced Voltage Pulsation in DC Winding of Five-Phase Wound-Field Switched Flux Machines," *IEEE Transactions on Energy Conversion*, vol. 34, no. 4, pp. 1890-1905, 2019. [CrossRef] [Google Scholar] [Publisher Link]

[28] Bakhtiar Khan et al., "Slot Filling Factor Calculation and Electromagnetic Performance of Single Phase Electrically Excited Flux Switching Motors," *The Applied Computational Electromagnetics Society Journal (ACES)*, vol. 35, no. 8, pp. 922-928, 2020. [CrossRef] [Google Scholar] [Publisher Link]

[29] Z.Q. Zhu, and J.T. Chen, "Advanced Flux-Switching Permanent Magnet Brushless Machines," *IEEE Transactions on Magnetics*, vol. 46, no. 6, pp. 1447-1453, 2010. [CrossRef] [Google Scholar] [Publisher Link]

[30] Xiaoyong Zhu et al., "Design and Multicondition Comparison of Two Outer-Rotor Flux-Switching Permanent Magnet Motors for In-Wheel Traction Applications," *IEEE Transactions on Industrial Electronics*, vol. 64, no. 8, pp. 6137-6148, 2017. [CrossRef] [Google Scholar] [Publisher Link]

[31] Hui Yang et al., "A Variable-Flux Hybrid-PM Switched-Flux Memory Machine for EV/HEV Applications," *IEEE Transactions on Industry Applications*, vol. 52, no. 3, pp. 2203-2214, 2016. [CrossRef] [Google Scholar] [Publisher Link]

[32] Zixuan Xiang et al., "Optimization Design and Analysis of a Hybrid Permanent Magnet Flux-Switching Motor with Compound Rotor Configuration," *CES Transactions on Electrical Machines and Systems*, vol. 2, no. 2, pp. 200-206, 2018. [CrossRef] [Google Scholar] [Publisher Link]

[33] Z.Z. Wu, and Z.Q. Zhu, "Analysis of Air-Gap Field Modulation and Magnetic Gearing Effects in Switched Flux Permanent Magnet Machines," *IEEE Transactions on Magnetics*, vol. 51, no. 5, pp. 1-12, 2015. [CrossRef] [Google Scholar] [Publisher Link]

[34] Mu Chen et al., "Cost-Effectiveness Comparison of Coaxial Magnetic Gears with Different Magnet Materials," *IEEE Transactions on Magnetics*, vol. 50, no. 2, pp. 821-824, 2014. [CrossRef] [Google Scholar] [Publisher Link]

[35] Mu Chen et al., "Development of Non-Rare-Earth Magnetic Gears for Electric Vehicles," *Journal of Asian Electric Vehicles*, vol. 10, no. 2, pp. 1607-1613, 2012. [CrossRef] [Google Scholar] [Publisher Link]

[36] Vanna Torn et al., "Performance Improvement of Flux Switching Permanent Magnet Wind Generator Using Magnetic Flux Barrier Design," *Sustainability*, vol. 15, no. 11, pp. 1-14, 2023. [CrossRef] [Google Scholar] [Publisher Link]

[37] Xiaohong Xue et al., "Design of Five-Phase Modular Flux-Switching Permanent-Magnet Machines for High-Reliability Applications," *IEEE Transactions on Magnetics*, vol. 49, no. 7, pp. 3941-3944, 2013. [CrossRef] [Google Scholar] [Publisher Link]

[38] N. Bianchi, and S. Bolognani, "Design Techniques for Reducing the Cogging Torque in Surface-Mounted PM Motors," *IEEE Transactions on Industry Applications*, vol. 38, no. 5, pp. 1259-1265, 2002. [CrossRef] [Google Scholar] [Publisher Link]

[39] K. Atallah, Jiabin Wang, and D. Howe, "Torque-Ripple Minimization in Modular Permanent-Magnet Brushless Machines," *IEEE Transactions on Industry Applications*, vol. 39, no. 6, pp. 1689-1695, 2003. [CrossRef] [Google Scholar] [Publisher Link]